

1 **pyControl: Open source, Python based, hardware and software for** 2 **controlling behavioural neuroscience experiments.**

3 Thomas Akam^{1,2*}, Andy Lustig³, James Rowland⁴, Sampath K.T. Kapaniah⁵, Joan Esteve-Agraz⁶,
4 Mariangela Panniello^{4,7}, Cristina Marquez⁶, Michael Kohl^{4,7}, Dennis Kätzel⁵, Rui M. Costa^{†,2,8}, Mark
5 Walton^{†,1}

6 1. Department of Experimental Psychology, University of Oxford, Oxford, UK

7 2. Champalimaud Neuroscience Program, Champalimaud Centre for the Unknown, Lisbon, Portugal

8 3. Janelia Research Campus, Howard Hughes Medical Institute, Ashburn, VA, USA

9 4. Department of Physiology Anatomy & Genetics, University of Oxford, Oxford, UK

10 5. Institute of Applied Physiology, Ulm University, Germany

11 6. Instituto de Neurociencias (Universidad Miguel Hernández-Consejo Superior de Investigaciones
12 Científicas), Sant Joan d'Alacant, Spain

13 7. Institute of Neuroscience and Psychology, University of Glasgow, Glasgow, UK

14 8. Department of Neuroscience and Neurology, Zuckerman Mind Brain Behavior Institute, Columbia
15 University, New York, NY, USA.

16 † Equal contribution.

17 * thomas.akam@psy.ox.ac.uk

18 **Abstract**

19 Laboratory behavioural tasks are an essential research tool. As questions asked of behaviour
20 and brain activity become more sophisticated, the ability to specify and run richly structured
21 tasks becomes more important. An increasing focus on reproducibility also necessitates
22 accurate communication of task logic to other researchers. To these ends we developed
23 pyControl, a system of open source hardware and software for controlling behavioural
24 experiments comprising; a simple yet flexible Python-based syntax for specifying tasks as
25 extended state machines, hardware modules for building behavioural setups, and a graphical
26 user interface designed for efficiently running high throughput experiments on many setups in
27 parallel, all with extensive online documentation. These tools make it quicker, easier and
28 cheaper to implement rich behavioural tasks at scale. As important, pyControl facilitates
29 communication and reproducibility of behavioural experiments through a highly readable task
30 definition syntax and self-documenting features.

31 **Resources**

32 Documentation: <https://pycontrol.readthedocs.io>

33 Repositories: <https://github.com/pyControl>

34 User support: <https://groups.google.com/g/pycontrol>

35 Introduction

36 Animal behaviour is of fundamental scientific interest, both in its own right and in relation to
37 brain function (Krakauer et al., 2017). Though understanding natural behaviour is the ultimate
38 goal, the tight control offered by laboratory tasks remains an essential tool in characterising
39 learning mechanisms. To serve the needs of contemporary neuroscience, hardware and
40 software for controlling behavioural experiments should be both flexible and easy to use.
41 Additionally, an increasing focus on reproducibility (Baker, 2016; International Brain
42 Laboratory et al., 2020) necessitates that behaviour control systems facilitate communication
43 and replication of behavioural paradigms across labs.

44 Available commercial solutions often fall short of these desiderata. Proprietary closed-source
45 hardware and software make it difficult to extend or adapt functionality beyond explicitly
46 implemented use cases. Additionally, programming behavioural tasks on commercial systems
47 can be surprisingly non-user-friendly, perhaps due to limitations of underlying legacy
48 hardware. Commercial hardware is also typically very expensive considering the level of
49 technology it represents, disadvantaging researchers outside well-funded institutions (Marder,
50 2013; Chagas, 2018), and constraining the ability to scale behavioural assays for high
51 throughput.

52 For these reasons, many groups implement their own behavioural hardware, either using low
53 cost microcontrollers such as Arduinos or raspberry PI, or generic laboratory control software
54 such as Labview (Devarakonda et al., 2016; O'Leary et al., 2018; Gurley, 2019; Bhagat et al.,
55 2020; Buscher et al., 2020). Though highly flexible, building behavioural control systems from
56 scratch has some disadvantages. It results in much duplication of effort as a lot of the required
57 functionality is generic across experiments. Additionally, unless custom systems are well
58 documented, it is hard for users to meaningfully share experimental protocols. This is
59 important because scientific publications do not consistently contain sufficient information to
60 constrain the details of the task used, yet such details are often crucial for reproducing the
61 behaviour. Making task code public is therefore key to reproducibility, but this is only effective
62 if it is readable and documented, as well as functional.

63 To address these limitations, we developed *pyControl*; a system of open source hardware and
64 software for controlling behavioural experiments. We report the design and rationale of
65 system components, validation experiments characterising system performance, and
66 behavioural data illustrating applications in 3 widely used, contrasting behavioural paradigms:
67 the 5-choice serial reaction time task (5-CSRTT) in operant chambers, sensory discrimination
68 in head fixed animals, and a social decision-making task in a maze apparatus.

69

70 **Results**

71 *System overview*

72 pyControl consists of three components, the pyControl framework, hardware, and graphical
73 user interface (GUI). The framework implements the syntax used to program behavioural
74 tasks. User-created task definition files, written in Python, run directly on microcontroller
75 hardware, supported by framework code that determines when user-defined functions are
76 called. This takes advantage of [Micropython](#), a recently developed port of the popular high-
77 level language Python to microcontrollers. The framework handles functionality that is
78 common across tasks, such as monitoring inputs, setting and checking timers, and streaming
79 data back to the computer. This minimises boilerplate code in task files, while ensuring that
80 common functionality is implemented reliably and efficiently. Combined with Python's highly
81 readable syntax, this results in task files that are quick and straightforward to write, but also
82 easy to read and understand (Figure 1), promoting replicability and communication of
83 behavioural experiments.

84 pyControl hardware consists of a breakout board which interfaces a pyboard microcontroller
85 with ports and connectors, and a set of devices such as nose-pokes, audio boards, LED
86 drivers, rotary encoders, and stepper motor controllers that are connected to the breakout
87 board to create behavioural setups. Breakout boards connect to the computer via USB.
88 Multiple breakout boards can be connected to a single computer, each controlling a separate
89 behavioural setup. pyControl implements a simple but robust mechanism for synchronising
90 data with other systems such as cameras or physiology hardware. All hardware is fully open
91 source, assembled hardware is available at low cost from the [Open Ephys store](#).

92 The GUI provides a graphical interface for setting up and running experiments, visualising
93 behaviour and configuring setups, and is designed to facilitate high-throughput behavioural
94 testing on many setups in parallel. To promote replicability, the GUI implements self-
95 documenting features which ensure that all task files used to generate data are stored with
96 the data itself, and that any changes to task parameters from default values are recorded in
97 the data files.

98 *Task definition syntax*

99 Here we give an overview of the task definition syntax and how this contributes to the flexibility
100 of the system. Detailed information about task programming is provided in the documentation
101 and set of example tasks is included with the GUI, including probabilistic reversal learning and
102 random ratio instrumental conditioning.

```
from pyControl.utility import *
from devices import *

# Define hardware

button = Digital_input('X1', rising_event='button_press')
LED     = Digital_output('X2')

# States and events.

states = ['LED_on',
         'LED_off']

events = ['button_press']

initial_state = 'LED_off'

# Variables

v.press_n = 0

# State behaviour functions.

def LED_off(event):
    if event == 'button_press':
        v.press_n = v.press_n + 1
        print('Press number {}'.format(v.press_n))
        if v.press_n == 3:
            goto_state('LED_on')

def LED_on(event):
    if event == 'entry':
        LED.on()
        timed_goto_state('LED_off', 1*second)
        v.press_n = 0
    elif event == 'exit':
        LED.off()
```

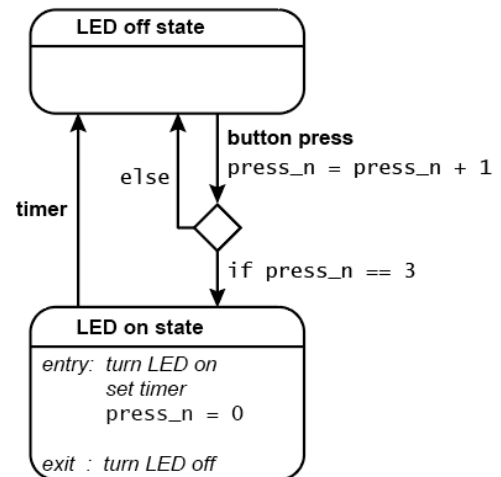


Figure 1. Example task. Complete task definition code (left panel) and corresponding state diagram (right panel) for a simple task that turns an LED on for 1 second when a button is pressed three times. Detailed information about the task definition syntax is provided in the [Programming Tasks](#) documentation.

103 pyControl tasks are implemented as state machines, the basic elements of which are states
104 and events. At any given time, the task is in one of the states, and the current state determines
105 how the task responds to events. Events may be generated externally, for example by the
106 subject's actions, or internally by timers.

107 Figure 1 shows the complete task definition code and the corresponding state diagram for a
108 simple task in which pressing a button 3 times turns on an LED for 1 second. The code first
109 defines the hardware that will be used, lists the task's state and event names, specifies the
110 initial state, and initialises task variables.

111 The code then specifies task behaviour by defining a *state behaviour function* for each state.
112 Whenever an event occurs, the state behaviour function for the current state is called with the
113 event name as an argument. Special events called *entry* and *exit* occur when a state is
114 entered and exited allowing actions to be performed on state transitions. State behaviour
115 functions typically comprise a set of *if* and *else if* statements that determine what happens

116 when different events occur in that state. Any valid Micropython code can be placed in a state
117 behaviour function, the only constraint being that it must execute fast as it will block further
118 state machine behaviour while executing. Users can define additional functions and classes
119 in the task definition file that can be called from state behaviour functions. For example, code
120 implementing a reversal learning task's block structure might be separated from the state
121 machine code in a separate function, improving readability and maintainability.

122 As should be clear from the above, while pyControl makes it easy to specify state machines,
123 tasks are not strict finite state machines, in which the response to an event depends *only* on
124 the current state, but rather extended state machines in which variables and arbitrary code
125 can also determine behaviour.

126 We think this represents a good compromise between enforcing a specific structure on task
127 code, which promotes readability and reliability and allows generic functionality to be efficiently
128 implemented by the framework, while allowing users enough flexibility to compactly define a
129 diverse range of complex tasks.

130 A key framework component is the ability to set timers to trigger state transitions or events.
131 The *timed_goto_state* function, used in the example, triggers a transition to a specified state
132 after a specified delay. Other functions allow timers to trigger a specified event after a
133 specified delay, or to cancel, pause and un-pause timers that have already been set.

134 To make things happen in parallel with the main state set of the task, the user can define an
135 *all_states* function which is called, with the event name as an argument, whenever an event
136 occurs irrespective of the state the task is in. This can be used in combination with timers and
137 variables to implement task behaviour that occurs independently from or interacts with the
138 main state set. For example to make something happen after a specified duration, irrespective
139 of the current state, the user can set a timer to trigger an event after the required duration, and
140 use the *all_states* function to perform the required action whenever the event occurs.

141 pyControl provides a set of functions for generating random variables, and maths functions
142 are available via the Micropython maths module. Though Micropython implements a large
143 subset of the core Python language (see the [Micropython docs](#)), it is not possible to use
144 packages such as *Numpy* or *Scipy* as they are too large to fit on a microcontroller.

145 *Framework implementation*

146 The pyControl framework consists of approximately 1000 lines of Python code. Figure 2
147 shows a simplified diagram of information flow between system components. Hardware inputs
148 and elapsing timers place events in a queue where they await processing by the state
149 machine. When events are processed, they are placed in a data output queue along with any

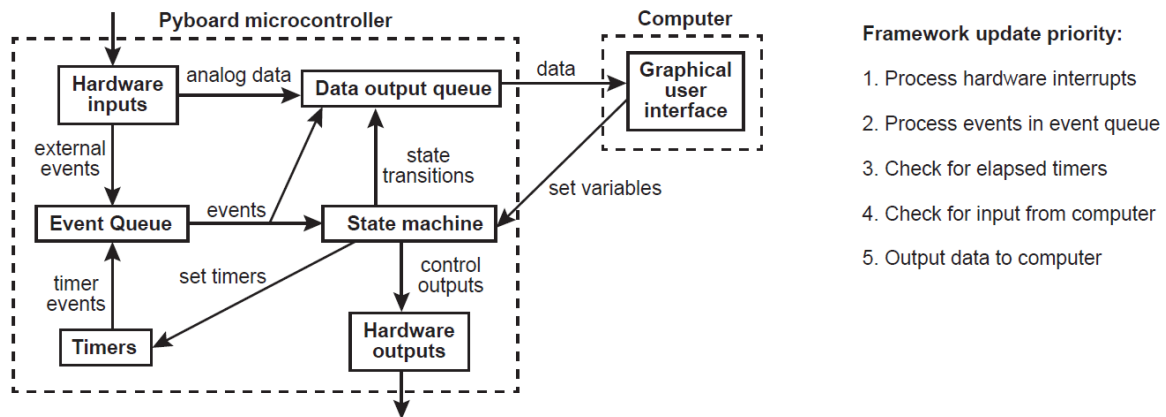


Figure 2. Framework diagram. Diagram showing the flow of information between different components of the framework and the GUI while a task is running. Right panel shows the priority with which processes occur in the framework update loop.

150 state transitions and user print statements that they generate. This design allows different
151 framework update processes to be prioritised by urgency, rather than by the order in which
152 they become necessary, ensuring the framework responds at low latency even under heavy
153 load (see validation experiments below). Top priority is given to processing hardware
154 interrupts, secondary priority to passing events from the event queue to the state machine and
155 processing their consequences, lowest priority to sending and receiving data from the
156 computer.

157 Digital inputs are detected by hardware interrupts and can be configured to generate separate
158 framework events on rising and/or falling edges. Analog inputs can stream continuous data
159 to the computer and trigger framework events when the signal goes above and/or below a
160 specified threshold.

161 *Hardware*

162 A typical pyControl hardware setup consists of a computer running the GUI, connected via
163 USB to one or more breakout boards, each of which controls a single behavioural setup
164 (Figure 3A). As task code runs on the microcontroller, the computer does not need to be
165 powerful. We typically use standard office desktops running Windows. We have not
166 systematically tested the maximum number of setups that can be controlled from one
167 computer but have run 24 in parallel without issue.

168 The breakout board interfaces a pyboard microcontroller (an Arm Cortex M4 running at
169 168MHz with 192KB RAM) with a set of *behaviour ports* used to connect devices that make
170 up behavioural setups, and BNC connectors, indicator LEDs and user pushbuttons (Figure
171 3B). Each behaviour port is an RJ45 connector (compatible with standard network cables)
172 with power lines (ground, 5V, 12V), two digital inputs/output (DIO) lines that are directly

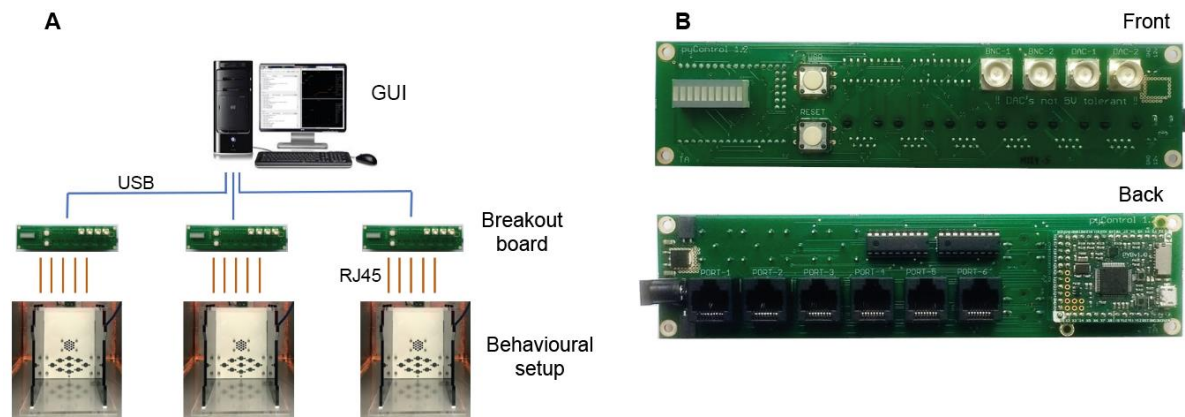


Figure 3. pyControl hardware. **A)** Diagram of a typical pyControl hardware setup, a single computer connects to multiple breakout boards, each of which controls one behavioural setup. Each behavioural setup is comprised of devices connected to the breakout board RJ45 behaviour ports using standard network cables. **B)** Breakout board interfacing the pyboard microcontroller with a set of behaviour ports, BNC connectors, indicator LEDs and user buttons. See supplementary figures S2-4 for hardware configurations used in the behavioural experiments reported in this manuscript, along with their associated hardware definition files. For more information see the [hardware docs](#).

173 connected to microcontroller pins, and two driver lines for switching higher current loads. The
174 driver lines are low side drivers (i.e. they connect the negative side of the load to ground) that
175 can switch currents up to 150mA at voltages up to 12V, with clamp diodes to the 12V rail to
176 support inductive loads such as solenoids. Two ports have an additional driver line and two
177 have an additional DIO. Six of the behaviour port DIO lines can alternatively be used as
178 analog inputs and two as analog outputs. Three ports support UART and two support I2C
179 serial communication over their DIO lines.

180 A variety of devices have been developed that connect to the ports, including nose-pokes,
181 levers, audio boards, rotary encoders, stepper motor drivers, lickometers and LED drivers
182 (Figures S2-4). Each has its own driver file that defines a Python class for controlling the
183 device. For detailed information about devices see the [hardware docs](#). The hardware
184 repository also contains open source designs for operant boxes and sound attenuating
185 chambers.

186 Though it is possible to specify the hardware that will be used directly in a task file as shown
187 in figure 1, it is typically done in a separate hardware definition file that is imported by the task.
188 This avoids redundancy when many tasks are run on the same setup. Additionally, abstracting
189 devices used in a task from the specific pins/ports they are connected to, allows the same task
190 to run on different setups as long as their hardware definitions instantiate the required devices.
191 See figures S2-4 for hardware definitions and corresponding hardware diagrams for the
192 example applications detailed below.

193 The design choice of running tasks on a microcontroller, and the specific set of devices
194 developed to date, impose some constraints on experiments supported by the hardware. The
195 limited computational resources preclude generating complex visual stimuli, making pyControl
196 unsuitable for most visual physiology in its current form. The devices for playing audio are
197 aimed at general behavioural neuroscience applications, and may not be suitable for some
198 auditory neuroscience applications. One uses the pyboard's internal DAC for stimulus
199 generation, and hence is limited to simple sounds such as sine waves or noise. Another plays
200 WAV files from an SD card, allowing for diverse stimuli but limited to 44KHz sample rate.

201 To extend the functionality of pyControl to application not supported by the existing hardware,
202 it is straightforward to interface setups with user created or commercial devices. This requires
203 creating an electrical connection between the devices and defining the inputs and outputs in
204 the hardware definition. Triggering external hardware from pyControl, or task events from
205 external devices, is usually achieved by connecting the device to a BNC connector on the
206 breakout board, and using the standard pyControl digital input or output classes. More
207 complex interactions with external devices may involve multiple inputs and outputs and/or
208 serial communication. In this case the electrical connection is typically made to a behaviour
209 port, as these carry multiple signal lines. A port adapter board, which breaks out an RJ45
210 connector to a screw terminal, simplifies connecting wires. Alternatively, if more complex
211 custom circuitry is required, e.g. to interface with a sensor, it may make sense to design a
212 custom printed circuit board with an RJ45 connector, similar to existing pyControl devices, as
213 this is more scalable and robust than implementing the circuit on a breadboard. To simplify
214 instantiating devices comprising multiple inputs and outputs, or controlling devices which
215 require dedicated code, users can define a Python class representing the device. These are
216 typically simple classes which instantiate the relevant pyControl input and output objects as
217 attributes, and may have methods containing code for controlling the device, e.g. to generate
218 serial commands. More information is provided in the hardware docs, and the design files and
219 associated code for existing pyControl devices provide a useful starting point for new designs.
220 Alla Karpova's lab at Janelia Research Campus have independently developed and open
221 sourced several pyControl compatible devices ([Github](#)).

222 For neuroscience applications, straightforward and failsafe synchronisation between
223 behavioural data and other hardware such as cameras or physiology recordings is essential.
224 pyControl implements a simple but robust method for this. Sync pulses are sent from
225 pyControl to the other systems, which each record the pulse times in their own reference
226 frame. The pulse train has random inter-pulse intervals which ensures a unique match
227 between pulse sequences recorded on each system, so it is always possible to identify which
228 pulse corresponds to which even if pulses are missing (e.g. due to forgetting to turn a system

229 on until after the start of a session). This also makes it unambiguous whether two files come
230 from the same session in the event of a file name mix-up. A Python module is provided for
231 converting times between different systems using the sync pulse times recorded by each. For
232 more information see the [synchronisation docs](#).

233 *Graphical User Interface*

234 The GUI provides two ways of setting up and running tasks; the *Run task* and *Experiments*
235 tabs, as well as a *Setups* tab used to name and configure hardware setups.

236 The *Run task* tab allows the user to quickly upload and run a task on a single setup. It is
237 typically used for prototyping tasks and testing hardware, but can also be used to acquire data.
238 The values of task variables can be modified before the task is started or while the task is
239 running. During the run, a log of events, state entries, and user print statements is displayed,
240 and the events, states, and any analog signals are plotted live in scrolling plot panels.

241 The *Experiments* tab is used for running experiments on multiple setups in parallel, and is
242 designed to facilitate high-throughput experiments where multiple users run cohorts of animals
243 through a set of boxes. An experiment consists of a set of subjects run in parallel on the same
244 task. If different subjects need to be run in parallel on different tasks this can be achieved by
245 opening multiple instances of the GUI.

246 To configure an experiment the user specifies which subjects will run on which setups, and
247 the values of any variables that will be modified before the task starts. Variables can be set
248 to the same value for all subjects or for individual subjects. Variables can be specified as
249 *Persistent*, causing their value to be stored on the computer at the end of the session, and
250 subsequently set to the same value the next time the experiment is run. Variables can be
251 specified as *Summary*, causing their values to be displayed in a table at the end of the
252 framework run and copied to the clipboard in a format that can be pasted directly into a
253 spreadsheet, for example to record the number of trials and rewards for each subject.
254 Experiment configurations can be saved and subsequently loaded.

255 When an experiment is run, the experiments tab changes from the *configure experiment*
256 interface to a *run experiment* interface. The session can be started and stopped individually
257 for each subject or simultaneously for all subjects. While each setup is running, a log of
258 events, state entries, and user print statements is displayed, along with the current state, most
259 recent event and print statement (Figure 4). Variable values can be viewed and modified for
260 individual subjects during the session. A tabbed plot window can be opened showing live
261 scrolling plots of the events, states and analog signals for each subject, and individual

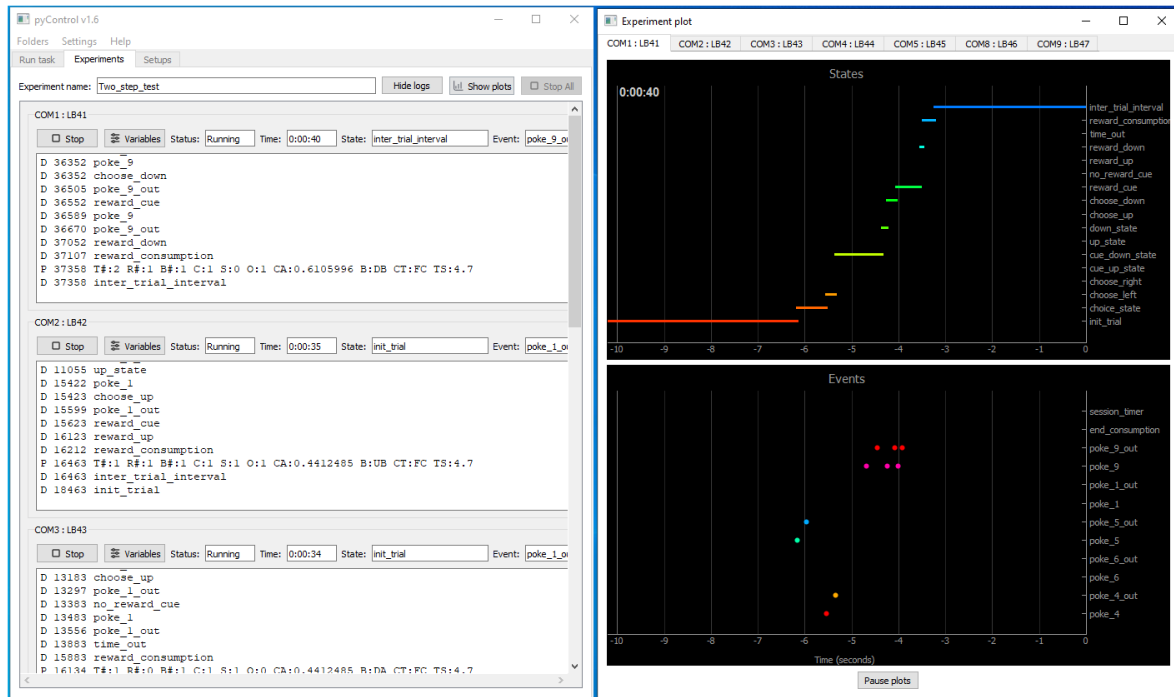


Figure 4. pyControl GUI. The GUI's *Experiments* tab is shown on the left running a multi-subject experiment, with the experiment's plot window open on the right showing the recent states and events for one subject. For images of the other GUI functionality see the [GUI docs](#).

262 subjects' plots can be undocked to allow behaviour of multiple subjects to be visualised
263 simultaneously.

264 The GUI is implemented entirely in Python using the PyQt GUI framework and PyQtGraph
265 plotting library. The GUI is cross platform and has been used on Windows, Mac and Linux,
266 though most development and testing has been under Windows. The code is organised into
267 modules for communication with the pyboard, different GUI components, and data
268 visualisation.

269 *pyControl data*

270 Data from pyControl sessions are saved as text files (see figure S1 for an example). When a
271 session starts, information including the subject, task and experiment names, and start data
272 and time, are written to the data file. While the task is running, all events and state transitions
273 are saved automatically with millisecond timestamps. The user can output additional data by
274 using the *print* function in their task file. This outputs the printed line to the computer, where
275 it is displayed in the log and saved to the data file, along with a timestamp. In decision making
276 tasks, we typically print one line each trial indicating the trial number, the subject's choice and
277 trial outcome, along with any other relevant task variables. If an error occurs while the
278 framework is running, a traceback reporting the error and line number in the task file where it

279 occurred is displayed in the log and written to the data file. Continuous data from analog inputs
280 is saved in separate binary files.

281 In addition to data files, task definition files used to generate data are copied to the
282 experiment's data folder, with a file hash appended to the file name that is also recorded in
283 the corresponding session's data file. This ensures that every task file version used in an
284 experiment is automatically saved with the data, and it is always possible to uniquely identify
285 the specific task file used for a particular session. If any variables are changed from default
286 values in the task file this is automatically recorded in the session's data file. These automatic
287 self-documenting features are designed to promote replicability of pyControl experiments. We
288 encourage users to treat the versioned task files as part of the experiment's data and include
289 them in data repositories.

290 Modules are provided for importing data files into Python for analysis and for visualising
291 sessions offline. Importing a data file creates a Session object with attributes containing the
292 session's information and data. For convenience, two representations of the state and event
293 data are generated; i) a dictionary whose keys are event and state names, and values are
294 numpy arrays with the corresponding event or state-entry times, and ii) a list of events and
295 state-entries in the order they occurred, whose elements are named tuples with the event/state
296 name and timestamp as attributes. For more information see the [data docs](#).

297 **Framework Performance**

298 To validate the performance of the pyControl framework we measured the system's response
299 latency and timing accuracy. Response latency was assessed using a task which set a digital
300 output to match the state of a digital input driven by a square wave signal. We recorded the
301 input and output signals and plot the distribution of latencies between the two signals across
302 all rising and falling edges (Figure 5A,B). In a 'low load' condition where the pyboard was not
303 processing other inputs, response latency was $556 \pm 17 \mu\text{s}$ (mean \pm SD). This latency reflects
304 the time to detect the change in the input, trigger a state transition, and update the output
305 during processing of the 'entry' event in the new state. We also measured response latency
306 in a 'high load' condition where the pyboard was additionally monitoring two digital inputs each
307 generating framework events in response to edges occurring as Poisson processes with an
308 average rate of 200 Hz, and acquiring signal from two analog inputs at 1 kHz sample rate
309 each. In this high load condition, the response latency was $859 \pm 241 \mu\text{s}$ (mean \pm SD), the
310 longest latency recorded was 3.3 ms with 99.6% of latencies < 2 ms.

311 To assess timing accuracy, we used a task which turned on a digital output for 10 ms when a
312 rising edge was received on a digital input. The input was driven by a 51 Hz square wave to
313 ensure that the timing of input edges drifted relative to the framework's 1ms clock ticks. We

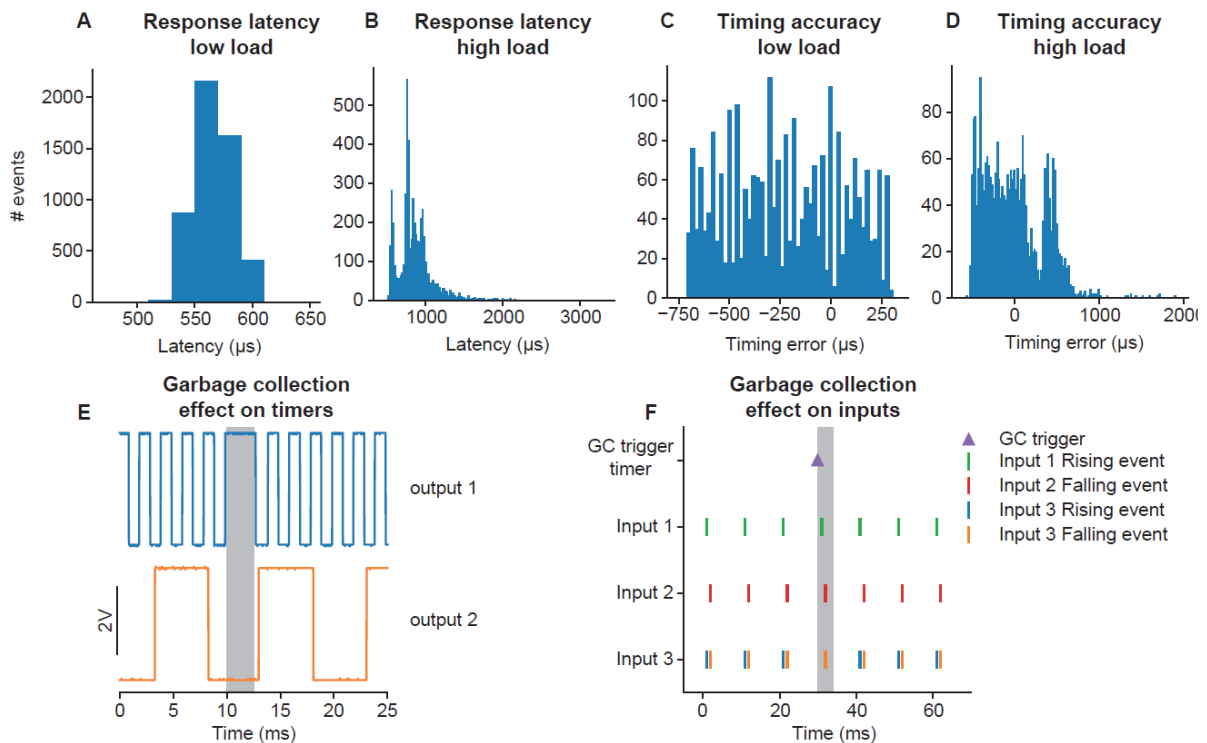


Figure 5. Framework Performance. **A)** Distribution of latencies for the pyControl framework to respond to a change in a digital input by changing the level of a digital output. **B)** As **A** but under a high load condition (see main text). **C)** Distribution of pulse duration errors when framework generates a 10ms pulse. **D)** As **C** but under a high load condition. **E)** Effect of Micropython garbage collection on pyControl timers. Signals are two digital outputs, one toggled on and off every 1ms (blue), and one every 5ms (orange), using pyControl timers. The 1ms timer that that elapsed during garbage collection (indicated by grey shading) was processed once garbage collection had finished, causing a short delay. Garbage collection had no effect on the 5ms timer that was running but did not elapse during garbage collection. **F)** Effect of garbage collection on pyControl inputs. A signal comprising 1ms pulses every 10ms was received by 3 pyControl digital inputs. Input 1 was configured to generated framework events on rising edges (green), input 2 on falling edges (red), and input 3 on both rising (blue) and falling (orange) edges. Garbage collection (indicated by grey shading) was triggered 1ms before an input pulse. Inputs 1 and 2 both generated their event that occurred during garbage collection with the correct timestamp. If multiple events occur on a single digital input during a single garbage collection, only the last event is generated correctly, causing the missing rising event on input 3.

314 plot the distribution of errors between the measured durations of the output pulses and the
 315 10ms target duration (Figure 5C,D). In the low load condition, timing errors were
 316 approximately uniformly distributed across 1 ms (mean error -220 μ s, SD 282 μ s), as expected
 317 given the 1ms resolution of the pyControl framework clock ticks. In the high load condition,
 318 timing variability was only slightly increased (mean -10 μ s, SD 353 μ s), with the largest
 319 recorded error 1.9 ms and 99.5% of errors <1 ms. Overall, these data show that the
 320 framework's latency and timing accuracy are sufficient for the great majority of neuroscience
 321 applications, even when operating under loads substantially higher than experienced in typical
 322 tasks.

323 Users who require very tight timing/latency performance should be aware of Micropython's
324 automatic garbage collection. Garbage collection is triggered when needed to free up memory
325 and takes a couple of milliseconds. Normal code execution is paused during garbage
326 collection, though interrupts (used to register external inputs and update the framework clock)
327 run as normal. pyControl timers that elapse during garbage collection are processed once it
328 has completed (Figure 5E). Timers that are running but do not elapse during garbage
329 collection are unaffected. Digital inputs that occur during garbage collection are registered
330 with the correct timestamp (Figure 5F), but will only be processed once garbage collection has
331 completed. The only situation where events may be missed due to garbage collection is if a
332 single digital input receives multiple event-triggering edges during a single garbage collection,
333 in which case only the last event is processed correctly (Figure 5F). To avoid garbage
334 collection affecting critical processing, the user can manually trigger garbage collection at a
335 time when it will not cause problems (see [Micropython docs](#)), for example during the inter-trial
336 interval. In the latency and timing accuracy validation experiments (Figure 5A-D), garbage
337 collection was triggered by the task code at a point in the task where it did not affect the
338 measurements.

339 A final constraint is that as each event takes time to process, there is a maximum *continuous*
340 event rate above which the framework cannot process events as fast as they occur, causing
341 the event queue to grow until available memory is exhausted. This rate will depend on the
342 processing triggered by each event, but is approximately 960Hz for digital inputs triggering
343 state transitions but no additional processing. In practice we have never encountered this
344 when running behavioural tasks as average event rates are typically orders of magnitude lower
345 and transiently higher rates are buffered by the queue.

346 **Application examples**

347 We illustrate how pyControl is used in practice with example applications in operant box, head-
348 fixed and maze-based tasks. Task and hardware definition files for these experiments are
349 provided in the manuscripts data repository. For additional use cases see also (Korn et al.,
350 2021; Akam et al., 2021; Koralek and Costa, 2020; Nelson et al., 2020; Blanco-Pozo et al.,
351 2021; van der Veen et al., 2021; Barros et al., 2021; Samborska et al., 2021; Kilonzo et al.,
352 2021; Strahnen et al., 2021).

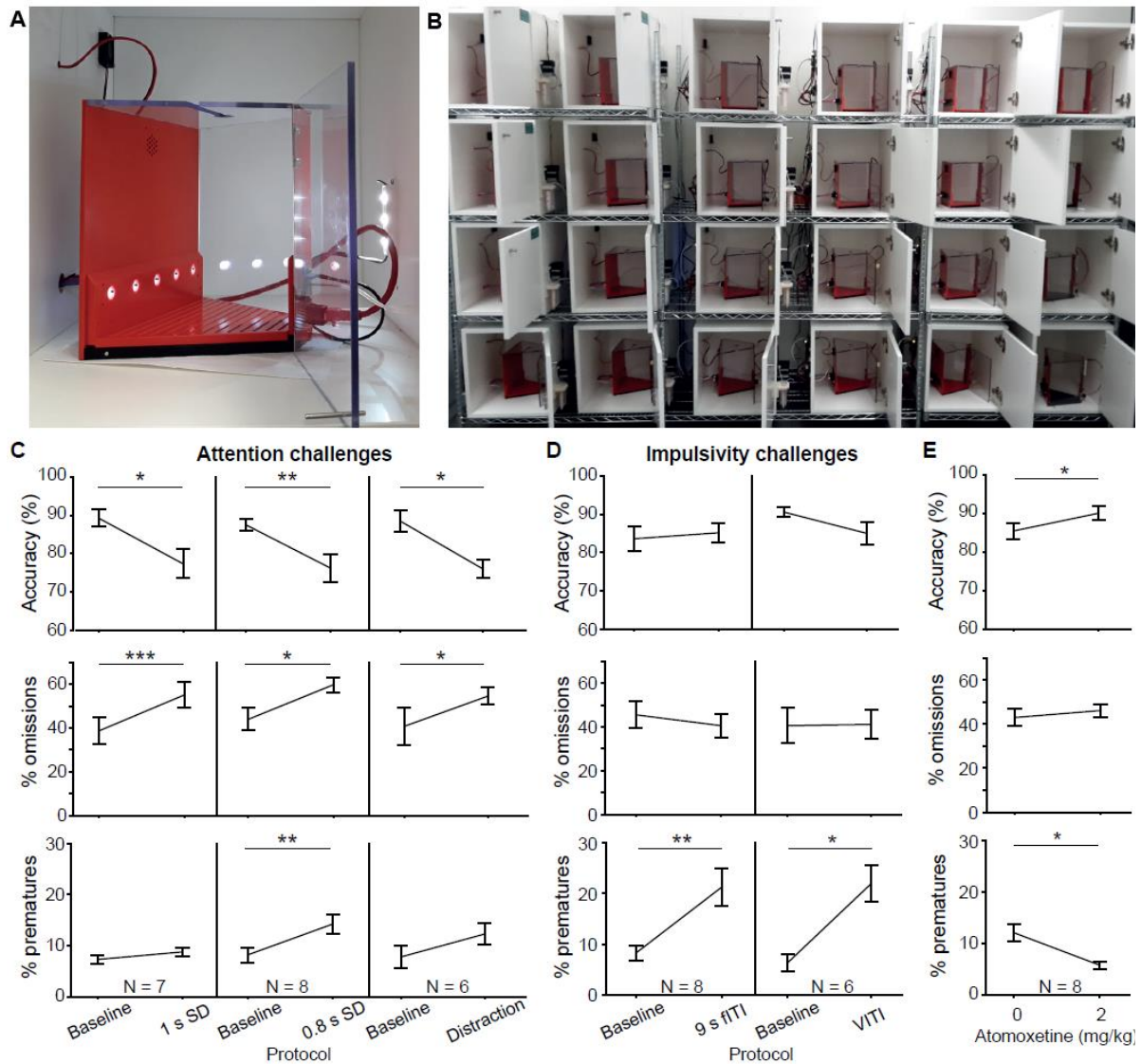


Figure 6. 5-choice serial reaction time task. **A)** Trapezoidal operant box with 5-choice wall (poke-holes shown illuminated) within a sound-attenuated cubicle. **B)** High throughput training setup comprising 24 operant boxes. **C, D)** Performance measures on the 5-CSRTT during protocols challenging either sustained attention - by shortening the SD or delivering a sound distraction during the waiting time (**C**) or motor impulsivity - by extending the ITI to a fixed (fITI) or variable (vITI) length (**D**). Protocols used are indicated by x-axes. Note the rather selective decrease of attentional performance (accuracy, %omissions) or impulse control (%prematures) achieved by the respective challenges. **E)** Validation of the possibility to detect cognitive enhancement in the 5-CSRTT (9s-fITI challenge) by application of atomoxetine, which increased attentional accuracy and decreased premature responding, as predicted. Asterisks in (**C-E**) indicate significant within-subject comparisons relative to the baseline (2 s SD, 5 s fITI; C-D) or the vehicle (**E**) condition (paired-samples t-test). * $P < 0.05$, * $P < 0.01$, * $P < 0.001$. Error bars display s.e.m. Note that two mice of the full cohort ($N = 8$) did not participate in all challenges as they required more training time to reach the baseline stage.

353 *5-choice serial reaction time task (5-CSRT)*

354 The 5-CSRT is a longstanding and widely used assay for measuring sustained visual attention
355 and motor impulsivity in rodents (Carli et al., 1983; Bari et al., 2008). The subject must detect
356 a brief flash of light presented pseudorandomly in one of five nose-poke ports, and report the
357 stimulus location by poking the port, to trigger a reward delivered to a receptacle on the
358 opposite wall.

359 We developed a custom operant box for the 5-CSRT (Figure 6 A,B), discussed in detail in a
360 separate manuscript (Kapaniah, Akam, Kätzel et al. in prep). The pyControl hardware
361 comprised a breakout board connected to a 5-poke board, which integrates the IR beams and
362 stimulus LEDs for the 5 choice ports on a single PCB, a single poke board for the reward
363 receptacle, an audio board, and a stepper motor board to control a peristaltic pump for reward
364 delivery (Figure S2).

365 To validate the setup, a cohort of 8 C57BL/6 mice was trained in the 5-CSRTT using a staged
366 training procedure (see Methods). The baseline protocol reached at the end of training used
367 a stimulus duration (SD) of 2 s and a 5 s inter-trial interval (ITI) from the end of reward
368 consumption to the presentation of the next stimulus. These task parameters were then
369 manipulated to challenge subject's ability to either maintain sustained attention, or withhold
370 impulsive premature responses. Attention was challenged in three conditions: by decreasing
371 the SD to either 1 s or 0.8 s, or by an auditory distraction of 70 dB white noise, played between
372 0.5 s and 4.5 s of the 5 s ITI. In all three attention challenges, the accuracy with which subjects
373 selected the correct port – the primary measure of sustained attention – decreased ($P < 0.05$;
374 paired t-tests comparing accuracy under the prior baseline protocol to accuracy under the
375 challenge condition, Figure 6C). Also, as expected, omissions (i.e. failures to poke any port in
376 the response window) increased ($P < 0.05$, t-test). In the attention challenges, the rate of
377 premature responses - the primary measure of impulsivity, remained either unchanged (1 s
378 SD challenge, auditory distraction; $P > 0.1$, t-test) or changed to a comparatively small extent
379 (0.8 s SD challenge, $P < 0.01$, t-test). Similarly, when impulsivity was challenged by extending
380 the ITI, to either a 9 s fixed ITI (fITI) or to a pseudo-randomly varied ITI length (vITI), premature
381 responses increased strongly ($P < 0.05$, t-test), while attentional accuracy and omissions did
382 not (Figure 6D). This specificity of effects of the challenges was as good – if not better – than
383 that achieved by us previously in a commercial set-up (Med Associates, Inc.) (Grimm et al.,
384 2018).

385 We further validated the task implementation by replicating effects of a pharmacological
386 treatment – atomoxetine - that has been shown to reduce impulsivity in the 5-CSRTT (Navarra
387 et al., 2008; Paterson et al., 2011). Using the 9 s fITI impulsivity challenge, we found that 2

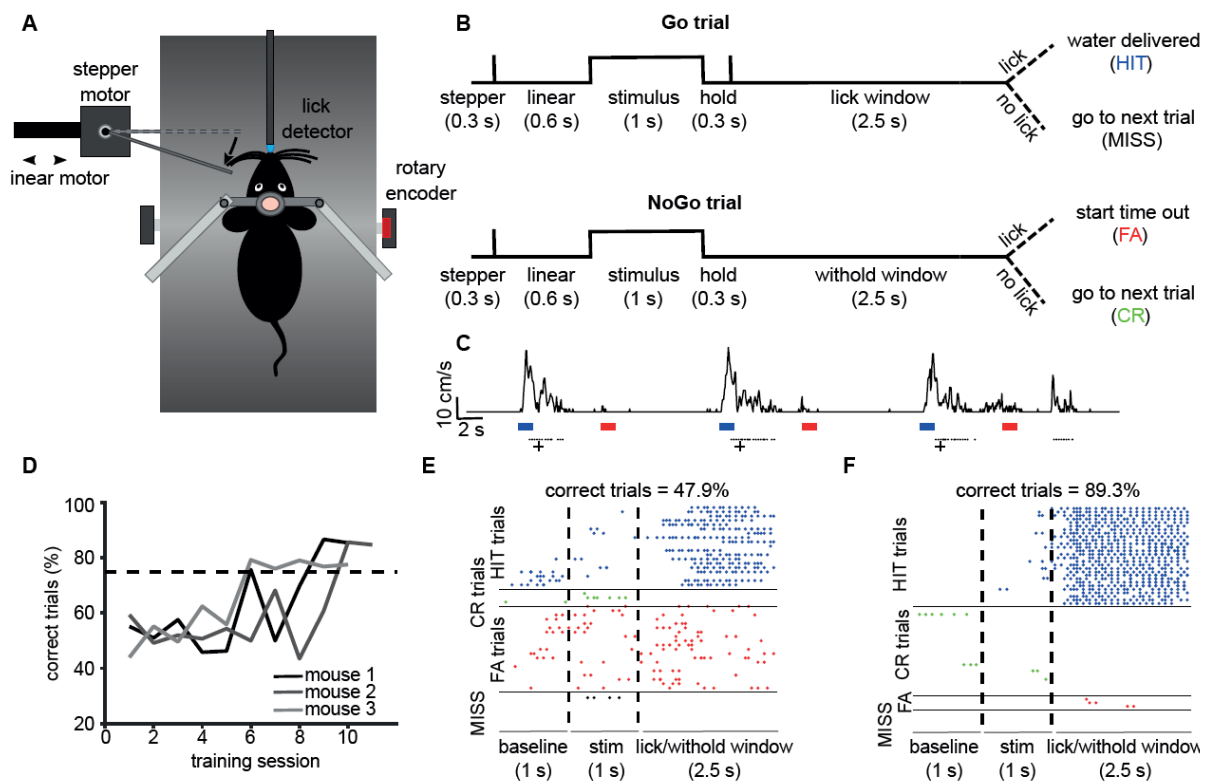


Figure 7. Vibrissae-based object localisation task. **A**) Diagram of the behavioural set up. Head-fixed mice were positioned on a treadmill with their running speed monitored by a rotary encoder. A pole was moved into the whisker field by a linear motor, with the anterior-posterior location controlled using a stepper motor. Water rewards were delivered via a spout positioned in front of the animal and licks to the spout were detected using an electrical lickometer. **B**) Trial structure: before stimulus presentation, the stepper motor moved into the trial position (anterior or posterior). Next, the linear motor translated the stepper motor and the attached pole close to the mouse's whisker pad, starting the stimulation period. A lick window (during Go trials), or withhold window (during NoGo trials) started after the pole was withdrawn. FA = false alarm; CR = correct rejection. **C**) pyControl simultaneously recorded running speed (top trace) and licks (black dots) of the animals, as well as controlling stimulus presentation (blue and red bars for Go and NoGo stimuli) and solenoid opening (black crosses). **D**) Percentage of correct trials for 3 mice over the training period. Mice were considered expert on the task after reaching 75% correct trials (dotted line) and maintaining such performance for 3 consecutive days. **E**) Detected licks before, during and after tactile stimulation, during an early session before the mouse has learned the task, sorted by trial type: HIT trials (blue), CORRECT REJECTION trials (green), FALSE ALARMS trials (red), and MISS trials (black). Each row is a trial, each dot is a detected lick. Correct trials for this session were 47.9% of total trials. **F**) As **E** but for data from the same mouse after reaching the learning threshold (correct trials = 89.3% of total trials).

388 mg/kg atomoxetine could reliably reduce premature responding and increase attentional
 389 accuracy ($P < 0.05$, paired t-test comparing performance under vehicle vs. atomoxetine;
 390 Figure 6E), consistent with its previously described effect in this rodent task (Navarra et al.,
 391 2008; Paterson et al., 2011; Pillidge et al., 2014; Fitzpatrick and Andreasen, 2019).

392

393 *Vibrissae-based object localisation task:*

394 We illustrate pyControl's utility for head-fixed behaviours with a version of the vibrissae-based
395 object localisation task (O'Connor et al., 2010). Head-fixed mice used their vibrissae
396 (whiskers) to discriminate the position of a pole moved into the whisker field at one of two
397 different anterior-posterior locations (Figure 7A). The anterior 'Go' location indicated that
398 licking in a response window after stimulus presentation would deliver a water reward, while
399 the posterior 'NoGo' location indicated that licking in the response window would trigger a
400 timeout (Figure 7B). Unlike in the original task mice were positioned on a treadmill allowing
401 them to run. Although running was not required to perform the task, we observed 10-20 s
402 running bouts alternated with longer stationary periods (Figure 7C), in line with previous
403 reports (Ayaz et al., 2019). pyControl hardware used to implement the setup comprised a
404 breakout board, a stepper motor driver to control the anterior-posterior position of the stimulus,
405 a lickometer, and a rotary encoder to measure running speed (Figure S3).

406 Mice were first familiarised with the experimental setup by head-fixing them on the treadmill
407 for increasingly long periods of time (5-20 min) over three days. From the fourth day, mice
408 underwent a "detection training", during which the pole was only presented in the Go position,
409 and water automatically delivered after each stimulus presentation. We then progressively
410 introduced NoGo trials, and made water delivery contingent on the detection of one or more
411 licks in the response window. Subjects reached 75% correct performance within five to nine
412 days from the first training session, at which point, they were trained for at least three further
413 days to make sure that they had reliably learned the task (Figure 7D). Early in training, mice
414 frequently licked prior to and during stimulus presentation, as well as during the response
415 window, on both Go and NoGo trials (Figure 7E). Following learning, licking prior to and during
416 stimulus presentation was greatly reduced, and mice licked robustly during the response
417 window on Go trials and withheld licking on NoGo trials, performing a high percentage of Hit
418 and Correct Rejection trials (Figure 7F).

419 *Social decision-making task:*

420 Our final application example is a maze-based social decision making task for mice, adapted
421 from that developed for rats by Márquez et al. (2015). In this task a 'focal' animal's choices
422 determine reward delivery for a 'recipient' animal, allowing preference for 'prosocial' vs 'selfish'
423 choices to be examined. The behavioural apparatus comprised an automated double T-maze
424 (Figure S4). Each T-maze consisted of a central corridor with nose-poke ports on each side
425 (choice area) and two side arms each with a food receptacle connected to a pellet dispenser
426 at the end (Figure 8A,B). Access from the central choice area to the side arms was controlled
427 by pneumatic doors.

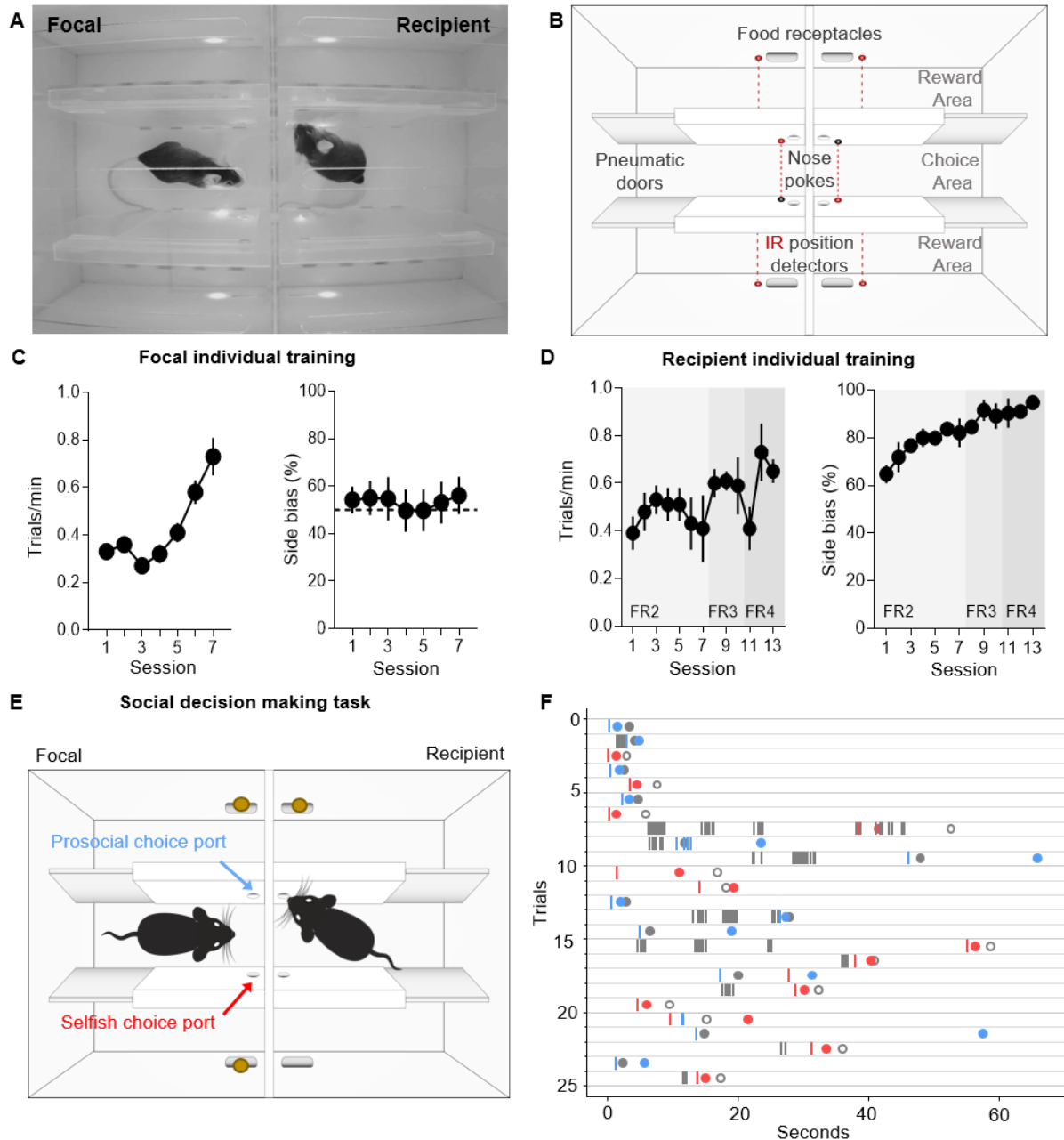


Figure 8. Social decision making task. **A)** Top view of double T maze apparatus showing two animals interacting during social decision making. **B)** Setup diagram; In each T maze, nose pokes are positioned on either side of the central choice area. Sliding pneumatic doors give access to the side arms of each maze (top and bottom in diagram) where pellet dispensers deliver food rewards. Six IR beams (depicted as grey and red circles connected by a dotted red line) detect the position of the animals to safely close the doors once access to an arm is secured. **C)** Focal animal individual training showing the number of trials completed per minute (left panel) and side bias (right panel) across days of training. **D)** As **C)** but for the recipient animal. **E)** Social decision making task. The trial starts with both animals in the central arm. The recipient animal has learnt in previous individual training to poke the port on the upper side of the diagram to give access to a food pellet in the corresponding reward area. During the social task the recipient animal's ports no longer control the doors but the animal can display food seeking behaviour by repeatedly poking the previously trained port. The focal animal has previously learned in individual training to collect food from the reward areas on both sides (top and bottom of diagram) by poking the corresponding port in the central choice area to activate the doors. During social decision making, the focal animal can either choose

the 'prosocial' port, giving both animals access to the side (upper on diagram) of their respective mazes where both receive reward, or can choose the 'selfish' port, giving both animals access to the other side (lower on diagram) where only the focal animal receives reward. **F)** Raster plot showing behaviour of a pair of animals over one session during early social testing. Nose pokes are represented by vertical lines, and colour coded according to the role of each mouse and choice type (grey – recipient's pokes, which are always directed towards the prosocial side, blue – focal's pokes in the prosocial choice port, red – focal's pokes in selfish port). Note that latency for focal choice varies depending on the trial, allowing the recipient to display its food seeking behaviour or not. Circles indicate the moment where each animal visits the food-receptacle in their reward arm. Focal animals are always rewarded, and the colour of the filled circle indicates the type of trial after decision (blue – prosocial choice, red – selfish choice). Grey circles indicate time of receptacle visit for recipients, where filled circles correspond to prosocial trials, where recipient is also rewarded, and open circles to selfish trials, where no pellet is delivered.

428 The task comprised two separate stages: (1) Individual training; where animals learn to open
429 doors by poking the ports in the central arms and retrieve pellets in the side arms. (2) Social
430 testing; where the decisions of the focal animal control the doors in both mazes, and hence
431 determine rewards for both itself and the recipient animal in the other maze.

432 The individual training protocols were different for the focal and recipient animals. During
433 individual training for the focal animal, a single poke in either port in the central arm opened
434 the corresponding door, allowing access to a side arm. Accessing either side arm was
435 rewarded with a pellet at the food receptacle in the arm. Under this schedule subjects
436 increased their rate of completing trials over 7 training days (Figure 8C, repeated measures
437 ANOVA $F(6,42)=12.566$ $p=0.000004$) without developing a bias for either side of the maze (P
438 > 0.27 for all animals, t-test). During individual training for the recipient animal, only one of
439 the nose-poke ports in the central arm was active, and the number of pokes required to open
440 the corresponding door increased over 13 days of training, with 4 pokes eventually required
441 to access the side arm to obtain a pellet in the food receptacle. Under this schedule the
442 recipient animals developed a strong preference for the active poke over the course of training
443 (Figure 8D right panel, repeated measures ANOVA $F(12,24)=3.908$ $p=0.002$), with
444 approximately 95% of pokes directed to the active side by the end of training.

445 During social testing, the two animals were placed in the double T-maze, one in each T,
446 separated by a transparent perforated partition that allowed the animals to interact using all
447 sensory modalities. The doors in the recipient animal's maze were no longer controlled by the
448 recipient animal's pokes, but were rather yoked to the doors of the focal animal, such that a
449 single poke to either port in the focal animals choice area opened the doors in both mazes on
450 the corresponding side. As in individual training, the focal animal was rewarded for accessing
451 either side, while the recipient animal was rewarded only when it accessed one side of the
452 maze. The choice made by the focal animal therefore determined whether the recipient animal
453 received reward, so the focal animal could either make 'pro-social' choices which rewarded

454 both it and the recipient, or ‘selfish’ choices which rewarded only the focal animal. As a proof
455 of concept, we show nose pokes and reward deliveries from a pair of interacting mice from
456 one social session (Figure 8F). A full analysis of the social behaviour in this task will be
457 published separately (Esteve-Agraz and Marquez, in preparation).

458 **Discussion**

459 pyControl is an open source system for running behavioural experiments, whose principal
460 strengths are: 1. a flexible and intuitive Python based syntax for programming tasks. 2.
461 Inexpensive, simple and extensible behavioural hardware that can be purchased commercially
462 or assembled by the user. 3. A GUI designed for efficiently running high throughput
463 experiments on many setups in parallel from a single computer. 4. Extensive online
464 documentation and user support.

465 pyControl can contribute to behavioural neuroscience in two important ways: First, it makes it
466 quicker, easier and cheaper to implement a wide range of behavioural tasks and run them at
467 scale. Second, it facilitates communication and reproducibility of behavioural experiments,
468 both because the task definition syntax is highly readable, and because self-documenting
469 features ensure that the exact task version and parameters used to generate data are
470 automatically stored with the data itself.

471 pyControl’s strengths and limitations stem from underlying design choices. We will discuss
472 these primarily in relation to two widely used open source systems for experiment control in
473 neuroscience [Bpod](#) (Josh Sanders) and [Bonsai](#) (Lopes et al., 2015). Bpod is a useful point
474 of comparison as it is probably the most similar project to pyControl in terms of functionality
475 and implementation, Bonsai because it represents a very different but powerful formalism for
476 controlling experiments that is often complementary. Space constraints preclude detailed
477 comparison with other projects, but see (Devarakonda et al., 2016; O’Leary et al., 2018; Kim
478 et al., 2019; Gurley, 2019; Saunders and Wehr, 2019; Bhagat et al., 2020; Buscher et al.,
479 2020).

480 Both pyControl and Bpod provide a state-machine-based task definition syntax in a high-level
481 programming language, run the state machine on a microcontroller, have commercially
482 available open source hardware, graphical interfaces for controlling experiments, and are
483 reasonably mature systems with a substantial user base beyond the original developers.
484 Despite these commonalities, there are significant differences which it is useful for prospective
485 users to understand.

486 The first is that in pyControl, user created task definition code runs directly on a pyboard
487 microcontroller, supported by framework code that determines when user defined functions

488 are called. This contrasts with Bpod, where user code written in either Matlab (Bpod) or
489 Python (PyBpod) is translated into instructions passed to the microcontroller, which itself runs
490 firmware implemented in the lower-level language C++. These two approaches offer distinct
491 advantages and disadvantages.

492 Running user Python code directly on the microcontroller avoids separating the task logic into
493 two conceptually distinct levels – flexible code written in a high-level language that runs on the
494 computer, and the more constrained set of operations supported by the microcontroller
495 firmware. Our understanding of how this works in Bpod is that the high level user code
496 implements a loop over trials where each loop defines a finite state machine for the current
497 trial - specifying for each state which outputs are on, and which events trigger transitions to
498 which other states, then uploads this information to the microcontroller, runs the state machine
499 until it reaches an exit condition indicating the end of the trial, and finally receives information
500 from the microcontroller about what happened before starting the next trial's loop. The
501 microcontroller firmware implements some functionality beyond a strict finite state machine
502 formalism, including timers and event counters that are not tied to a particular state, but does
503 not support arbitrary user code or variables. We suggest readers consult the relevant
504 documentation ([pyControl](#), [Bpod](#), [PyBpod](#)) and example tasks ([pyControl](#), [Bpod](#), [pyBpod](#)) to
505 compare syntaxes directly. A second advantage of running user code directly on the
506 microcontroller is that the user has direct access from their task code to microcontroller
507 functionality such as serial communication. A third is that the pyControl framework (as well
508 as the GUI) is written in Python rather than C++, facilitating code maintenance, and lowering
509 the barrier to users extending system functionality.

510 The two principal disadvantages of running the task entirely on the microcontroller are: 1)
511 although modern microcontrollers are very capable, their resources are more limited than a
512 computer - which constrains how computationally and memory intensive task code can be and
513 precludes using modules such as Numpy. 2) Lack of access to the computer from task code,
514 for example to interact with other programs or display custom plots. To address these
515 limitations, we are currently developing an application programming interface (API) to allow
516 pyControl tasks running on the microcontroller to interact with user code running on the
517 computer. This will work via the user defining a Python class with methods that get called at
518 the start and end of the run for initial setup and post-run clean-up, as well as an update method
519 called regularly during the run with any new data received from the board as an argument.

520 There are also differences in hardware design. The two most significant are; 1) The pyControl
521 breakout board tries to make connectors (behaviour ports and BNC) as flexible as possible at
522 the cost of not being specialised for particular functions. Bpod tends to use a given connector

523 for a specific function - e.g. it has separate *behaviour ports* and *module ports*, with the former
524 designed for controlling a nose-poke, and the latter for UART serial communication with
525 external modules. Practically, this means that pyControl exposes microcontroller pins (which
526 often support multiple functions) directly on connectors whereas Bpod tends to incorporate
527 intervening circuitry such as electrical isolation for BNC connectors and serial line driver ICs
528 on module ports. 2) Bpod uses external modules, each with its own microcontroller and C++
529 firmware, for functions which pyControl implements using the microcontroller on the breakout
530 board, specifically; analog input and output, I2C serial communication, and acquiring signal
531 from a rotary encoder. These design choices make pyControl hardware simpler and cheaper.
532 Purchased commercially the Bpod state machine costs \$765, compared to €250 for the
533 pyControl breakout board, and Bpod external modules each cost hundreds of dollars. This is
534 not to say that pyControl necessarily represent better value; a given Bpod module may offer
535 more functionality (e.g. more channels, higher sample rates). But the two systems do
536 represent different design approaches.

537 Both the pyControl and pyBpod GUI's support configuring and running experiments on multiple
538 setups in parallel from a single computer, while the Matlab based Bpod GUI controls a single
539 setup at a time. Their user interfaces are each very different; the respective user guides
540 ([pyControl](#), [Bpod](#), [PyBpod](#)) give the best sense for the different approaches. We think it is a
541 strength of the pyControl GUI, reflecting the relative simplicity of the underlying code base,
542 that scientist users not originally involved in the development effort have made substantial
543 contributions to its functionality (see GitHub [pull requests](#)).

544 Bonsai (Lopes et al., 2015) represents a very different formalism for experiment control that is
545 not based around state machines. Instead, the Bonsai user designs a *dataflow* by arranging
546 and connecting nodes in a graphical interface, where nodes may represent data sources,
547 processing steps, or outputs. Bonsai can work with a diverse range of data types including
548 video, audio, analog and digital signals. Multiple data streams can be processed in parallel
549 and combined via a rich set of operators including arbitrary user code. Bonsai is very powerful,
550 and it is likely that any task implemented in pyControl could also be implemented in Bonsai.
551 The reverse is certainly not true, as Bonsai can perform computationally demanding real time
552 processing on high dimensional data such as video, which is not supported by pyControl.

553 Nonetheless, in applications where either system could be used, there are reasons why
554 prospective users might consider pyControl: 1) pyControl's task definition syntax may be more
555 intuitive for tasks where (extended) state machines are a natural formalism. The reverse is
556 true for tasks requiring parallel processing of multiple complex data streams. 2) pyControl is
557 explicitly designed for efficiently running high throughput experiments on many setups in

558 parallel. Though it is possible to control multiple hardware setups from a single Bonsai
559 dataflow, Bonsai does not explicitly implement the concept of a multi-setup experiment so the
560 user must duplicate dataflow components for each setup themselves. As task parameters
561 and data file names are specified across multiple nodes in the dataflow, configuring these for
562 a cohort of subjects can be laborious - though it is possible to automate this by calling Bonsai's
563 command line interface from user created Python scripts. 3) pyControl hardware modules can
564 simplify the physical construction of behavioural setups. Though Bonsai itself is software,
565 some compatible behavioural hardware has been developed by the Champalimaud
566 Foundation Hardware Platform (<https://www.cf-hw.org/harp>), which offers tight timing
567 synchronisation and close integration with Bonsai, though documentation is currently limited.
568 In practice, we think the two systems are often complementary; for example we use Bonsai in
569 our workflow for acquiring and compressing video data from sets of pyControl operant boxes
570 ([Github](#)), and we hope to integrate them more closely in future.

571 pyControl is under active development. We are currently prototyping a home-cage training
572 system which integrates a pyControl operant box with a mouse home-cage, via an access
573 control module which allows socially housed animals to individually access the operant box to
574 train themselves with minimal user intervention. We are also developing hardware to enable
575 much larger scale behavioural setups, such as complex maze environments with up to 68
576 behaviour ports per setup. As discussed above, we are finalising an API to allow pyControl
577 tasks to interact with user Python code running on the computer.

578 In summary, pyControl is a user friendly and flexible tool addressing a commonly encountered
579 use case in behavioural neuroscience; defining behavioural tasks as extended state
580 machines, running them efficiently as high throughput experiments, and communicating task
581 logic to other researchers.

582 **Acknowledgments**

583 T.A. thanks current and former members of the Champalimaud hardware and software
584 platforms; Jose Cruz, Ricardo Ribeiro, Carlos Mão de Ferro and Matthieu Pasquet for
585 discussions and technical assistance, and Filipe Carvalho and Lídia Fortunato of Open Ephys
586 Production Site for hardware assembly and distribution. C.M. thanks Victor Rodriguez for
587 assistance developing the social decision making apparatus. M.P. and M.K. thank Dr Ana
588 Carolina Bottura de Barros and Dr Severin Limal for assistance with the Vibrissae-based
589 object localisation task.

590 **Author Contributions**

591 Developed hardware: T.A. Developed software: T.A., A.L., J.R. Designed and ran behavioural
592 experiments: S.K., J.E-A, M.P, C.M, M.K, D.K. Wrote the manuscript: T.A, S.K., J.E-A, M.P,
593 C.M, M.K, D.K. Edited the manuscript: R.M.C., M.W.

594 **Competing Interests**

595 T.A. has a consulting contract with Open Ephys Production Site who sell assembled pyControl
596 hardware. The other authors have no competing interests to report.

Key Resources Table				
Reagent type (species) or resource	Designation	Source or reference	Identifiers	Additional information
Software	pyControl code	https://github.com/pyControl/code		Repository containing pyControl GUI and framework code.
Hardware	pyControl hardware	https://github.com/pyControl/hardware		Repository containing pyControl hardware designs
Documentation	pyControl Docs	https://pycontrol.readthedocs.io		pyControl documentation
Data	Data repository	https://github.com/pyControl/manuscript		Repository containing pyControl task files, data and analysis code associated with the manuscript.

597

598 **Methods**

599 pyControl task files used in all experiments, and data and analysis code for the performance
600 validation experiments, are included in the manuscript's [data and code repository](#).

601 *Framework performance validation*

602 Framework performance was characterised using pyboards running Micropython version 1.13
603 and pyControl version 1.6. Electrical signals used to characterise response latency and timing
604 accuracy (Figure 5) were recorded at 50 kHz using a Picoscope 2204A USB oscilloscope.

605 To assess response latency (Figure 5A,B), a pyboard running the task file *input_follower.py*
606 received a 51 Hz square wave input generate by the picoscope's waveform generator. The
607 task turned an output on and off to match the state of the input signal. The latency distribution
608 was assessed by recording 50 seconds of the input and output signals and evaluating the
609 latency between the signals at each rising and falling edge.

610 To assess timing accuracy (Figure 5C,D), a pyboard running the task file *triggered_pulses.py*
611 received a 51Hz square wave input generate by the picoscope's waveform generator. The
612 task triggered a 10ms output pulse whenever a rising edge occurred in the input signal. The
613 output signals was recorded for 50 s and the duration of each output pulses was measured to
614 assess the distribution of timing errors.

615 In both cases the experiments were performed separately in a low load and high load
616 condition. In the low load condition the task was not monitoring any other inputs. In the high
617 load condition, the task was additionally acquiring data from two analog inputs at 1 kHz sample
618 rate each, and monitoring two digital inputs, each of which was generating framework events
619 in response to edges occurring as a Poisson process with average rate 200 Hz. These
620 Poisson input signals were generated by a second pyboard running the task
621 *poisson_generator.py*.

622 To assess the effect of garbage collection on pyControl timers (Figure 5E), the task file
623 *gc_timer_test.py* was run on a pyboard. This uses pyControl timers to toggle one digital output
624 on and off every 1 ms and another every 5ms. The resulting signals were recorded using the
625 picoscope and plotted around a garbage collection episode identified by visually inspecting
626 the 1 ms timer signal.

627 To assess the effect of garbage collection on digital input processing (Figure 5F), a signal
628 comprising 1ms pulses every 10ms was generated using the picoscope, and connected to 3
629 digital inputs on a pyboard running the task *gc_inputs_test.py*. The task configures one input
630 to generate events on rising edges, one on falling edges and one on both rising and falling
631 edges, and uses a pyControl timer to trigger garbage collection 1ms before a subset of the
632 input pulses. Event times recorded by pyControl were plotted to generate the figure.

633 Analysis and plotting of the framework validation data was performed in Python using code
634 included in the data repository.

635 **Application examples**

636 *5 choice serial reaction time task:*

637 Animals

638 The 5-CSRTT experiment used a cohort of 8 male C57BL/6 mice, aged 3-4 months at the
639 beginning of training. Animals were group-housed (2-3 mice per cage) in Type II-Long
640 individually ventilated cages (Greenline, Tecniplast, G), enriched with sawdust, sizzle-nestTM,
641 and cardboard houses (Datesand, UK), and subjected to a 13 h light / 11 h dark cycle. Mice
642 were kept under food-restriction at 85-95% of their average free-feeding weight which was

643 measured over 3 d immediately prior to the start of food-restriction at the start of the
644 behavioural training. Water was available ad libitum.

645 This experiment was performed in accordance to the German Animal Rights Law
646 (Tierschutzgesetz) 2013 and approved by the Federal Ethical Review Committee
647 (Regierungspräsidium Tübingen) of Baden-Württemberg.

648 Behavioural hardware

649 The design of the operant boxes for the 5-CSRTT setups will be discussed in detail in a
650 separate manuscript (Kapaniah, Akam, Kätzel et al. in prep). Briefly, the box had a trapezoidal
651 floorplan with the 5 choice wall at the wide end and reward receptacle at the narrow end of
652 the trapezoid, to minimize the floor area and hence reduce distractions. The side-walls and
653 roof were made of transparent acrylic to allow observation of the animal, the remaining walls
654 were made from opaque PVC to minimize visual distractions (Figure 6a). Design files for the
655 operant box, and peristaltic and syringe pumps for reward delivery, are at
656 <https://github.com/KaetzelLab/Operant-Box-Design-Files>. Potentially distracting features
657 (house light, cables) were located outside of the box and largely invisible from the inside. The
658 pyControl hardware used and the associated hardware definition is shown in figure S2. The
659 operant box was enclosed by a sound attenuating chamber, custom made in 20mm melamine-
660 coated MDF, adapted from a design in the [hardware repository](#). The pyControl breakout
661 boards, and other PCBs that were not integrated into the box itself, were mounted on the
662 outside of the sound attenuating chamber, and a CCTV camera was mounted on the ceiling
663 to monitor behavior.

664 5-CSRTT training

665 The 5-CSRTT training protocol was similar to what we described previously (Grimm et al.,
666 2018; van der Veen et al., 2021). In brief, after initiation of food-restriction, mice were
667 accustomed to the reward (strawberry milk, Müllermilch™, G) in their home cage and in the
668 operant box (2-3 exposures each). Then, mice were trained on a simplified operant cycle in
669 which all holes of the 5-poke wall were illuminated for an unlimited time, and the mouse could
670 poke into any one of them to illuminate the reward receptacle on the opposite wall and
671 dispense a 40 µl milk reward. Once mice attained at least 30 rewards each in two consecutive
672 sessions, they were moved to the 5-CSRTT task.

673 During 5-CSRTT training, mice transitioned through five stages of increasing difficulty, based
674 on reaching performance criteria in each stage (Table 1). The difficulty of each stage was
675 determined by the length of time the stimulus was presented (stimulus duration, SD) and the

5-CSRTT training						
	Task Parameters		Criteria for stage transition (2 consecutive days)			
Stage	SD (s)	ITI (s)	# correct	% correct	% accuracy	% omissions
S1	20	2	>= 30	>= 40	-	-
S2	8	2	>= 40	>= 50	-	-
S3	8	5			>= 80	<= 50
S4	4	5			>= 80	<= 50
S5	2	5			>= 80	<= 50
Challenges						
C1	2	9	Impulsivity challenge			
C2	1	5	Attention challenge 1			
C3	0.8	5	Attention challenge 2			
C4	2	5	Distraction: 1s white noise within 0.5-4.5s of ITI			
C5	2	7, 9, 11, 13	Variable ITI: pseudo-random, equal distribution			

Table 1. 5-CSRTT Training and challenge stages. The parameters stimulus duration (SD) and intertrial-interval (ITI, waiting time before stimulus) are listed for each of the 5 training stages (S1-5) and the subsequent challenge protocols on which performance was tested for 1 day each (C1-5). For the training stages, performance criteria which had to be met by an animal on two consecutive days to move to the next stage are listed on the right. See Methods for the definition of these performance parameters.

676 length of the inter-trial interval (ITI) between the end of the previous trial and the stimulus
677 presentation on the next trial.

678 The ITI was initiated when the subject exited the reward receptacle after collection of a reward,
679 or by the end of a time-out period (see below). The ITI was followed by illumination of one hole
680 on the 5-choice wall for the SD determined by the training stage. A poke in the correct port
681 during the stimulus, or during a subsequent 2s hold period, was counted as a *correct*
682 *response*, illuminating the reward receptacle and dispensing 20 µl of milk. If the subject either
683 poked into any hole during the ITI (*premature response*), poked into a non-illuminated hole
684 during the SD or hold period (*incorrect response*), or failed to poke during the trial (*omission*),
685 the trial was not rewarded but instead terminated with a 5 s time-out during which the house
686 light was turned off. The relative numbers of each response type were used as performance
687 indicators measuring premature responding [$\%premature = 100 \times (\text{number of premature responses}) / (\text{number of trials})$],
688 sustained attention [$accuracy = 100 \times (\text{number of correct responses}) / (\text{number of correct and incorrect responses})$],
689 and lack of participation [$\%omissions = 100 \times (\text{number of omissions}) / (\text{number of trials})$]. In all stages and tests, sessions
690 lasted 30 min and were performed once daily at the same time of day.
691

692 Test days with behavioural challenges were interleaved with at least one training day on the
693 baseline stage (stage 5; see Table 1 for parameters of all stages). For pharmacological

694 validation, atomoxetine (Tomoxetine hydrochloride, Tocris, UK) diluted in sterile saline (0.2
695 mg/ml) or saline vehicle were injected i.p. at 10 μ l/g mouse injection volume 30 min before
696 testing started. For atomoxetine vs. vehicle within-subject comparison, two tests were
697 conducted separated by one week, whereby four animals received atomoxetine on the first
698 day, while the other four received vehicle and vice versa for the second day. Effects of
699 challenges (compared to performance on the prior day with baseline training) and atomoxetine
700 (compared to performance under vehicle) were assessed by paired-samples *t*-tests.
701 Behavioural data gathered in the 5-CSRTT was analysed with Excel and SPSS26.0 (IBM Inc.,
702 US).

703 *Vibrissae-based object localisation task:*

704 Animals

705 Subjects were three female mice expressing the calcium-sensitive protein GCaMP6s in
706 excitatory neurons, derived by mating the floxed Ai94(TITL-GCaMP6s)-D line (Jackson
707 Laboratories; stock number 024742) with the CamKII-tta (Jackson Laboratories; stock number
708 003010). Animal husbandry and experimental procedures were approved and conducted in
709 accordance with the United Kingdom Animals (Scientific Procedures) Act 1986 under project
710 license P8E8BBDAD and personal licenses from the Home Office.

711 Behavioural hardware

712 Mice were head-fixed on a treadmill fashioned from a 24 cm diameter Styrofoam cylinder
713 covered with 1.5 mm thick neoprene. An incremental optical encoder (Broadcom HEDS-
714 5500#A02; RS Components) was used in conjunction with a pyControl rotary encoder adapter
715 to monitor mouse running speed. The pole used for object detection was a blunt 18G needle
716 mounted, via a 3d-printed arm, onto a stepper motor (RS PRO Hybrid 535-0467; RS
717 Components). The stepper motor was mounted onto a motorized linear stage (DDSM100/M;
718 Thorlabs) used to move the pole toward and away from the whisker pad (controlled by a K-
719 Cube Brushless DC Servo Driver (KBD101; Thorlabs). The pyControl hardware used and the
720 associated hardware definition is shown in figure S3.

721 Surgery

722 6-10 week old mice were anaesthetised with isoflurane (0.8-1.2% in 1 L/min oxygen) and
723 implanted with custom titanium headplates for head-fixation and 4 mm diameter cranial
724 windows for imaging as described previously (Chong et al., 2019). Peri- and post-operative

725 analgesia was used (meloxicam 5mg/kg and buprenorphine 0.1 mg/kg) and mice were
726 carefully monitored for 7 days post-surgery.

727 Behavioural training

728 Following recovery from surgery, mice were habituated to head-fixation (Chong et al., 2019)
729 prior to training on the vibrissa-based object localisation task as detailed in the results section.
730 Data were analysed using MATLAB (Mathworks).

731 *Social decision making task:*

732 Animals

733 12 male C57BL6/J mice (Charles River, France) were used, aged 3 months at the beginning
734 of the experiment. Animals were group-housed (4 animals per cage) and maintained with ad
735 libitum access to food and water in a 12 – 12 h reversed light cycle (lights off at 8 am) at the
736 Animal Facility of the Instituto de Neurociencias of Alicante. Short food restrictions (2 h before
737 the behavioural testing) were performed in the early phases of individual training to increase
738 motivation for food-seeking behaviour, otherwise animals were tested with ab libitum chow
739 available in their home cage. All experimental procedures were performed in compliance with
740 institutional Spanish and European regulations, as approved by the Universidad Miguel
741 Hernández Ethics committee.

742 Behavioural hardware

743 The Social decision making task was performed in a double maze, where two animals, the
744 focal and the recipient, would interact and work to obtain food rewards. The outer walls of the
745 double maze were of white laser cut acrylic. Each double maze was divided by a transparent
746 and perforated wall creating the individual mazes for each mouse. For each individual maze,
747 inner walls separating central choice and side reward areas, contained the mechanisms for
748 sliding doors, 3D printed nose-pokes and position detectors. These inner walls were made of
749 transparent laser cut acrylic, in order to allow visibility of the animal in the side arms of the
750 maze. Walls of the central choice area were frosted to avoid reflections that could interfere
751 with automated pose estimation of the interacting animals in this area.

752 Each double T-maze behavioural setup was positioned inside a custom-made sound isolation
753 box, with an infra-red sensitive camera (PointGrey Flea3 -U3-13S2M CS, Canada) positioned
754 above the maze to track the animals' location. The chamber was illuminated with dim white
755 light (4 lux) and infra-red illumination located on the ceiling of the sound attenuating chamber.
756 The pyControl hardware configuration and associated hardware definition file are shown in

757 figure S4. Food pellet rewards were dispensed using pellet dispensers made of 3D printed
758 and laser cut parts actuated by a stepper motor (NEMA 42HB34F08AB, e-ika electrónica y
759 robótica, Spain) controlled by a pyControl stepper driver board, placed outside the sound
760 isolation box and delivering the pellets to the 3D printed food receptacles through a silicon
761 tube. Design files for the pellet dispenser and receptacles are at
762 <https://github.com/MarquezLab/Hardware>. The sliding doors that control access to the side
763 arms were actuated by pneumatic cylinders (Cilindro ISO 6432, Vestonn Pneumatic, Spain)
764 placed below the base of the maze, providing silent and smooth horizontal movement of the
765 doors. These were in turn controlled via solenoid valves (8112005201, Vestonn Pneumatic,
766 Spain) interfaced with pyControl using an optocoupled relay board (Cebek- T1, Fadisel,
767 Spain). The speed of the opening/closing of the doors could be independently regulated by
768 adjusting the pressure of the compressed air to the solenoid valves.

769 Behavioural training

770 Individual training and social decision making protocols are described in the results section.
771 All behavioural experiments and were performed during the first half of the dark phase of the
772 cycle. Data were analysed with Python (Python Software Foundation, v3.6.5) and statistical
773 analysis performed with IBM SPSS Statistics (version 26).

774 **References**

- 775 Akam, T., Rodrigues-Vaz, I., Marcelo, I., Zhang, X., Pereira, M., Oliveira, R.F., Dayan, P.,
776 and Costa, R.M. (2021). The Anterior Cingulate Cortex Predicts Future States to Mediate
777 Model-Based Action Selection. *Neuron* 109, 149-163.e7.
- 778 Ayaz, A., Stäuble, A., Hamada, M., Wulf, M.-A., Saleem, A.B., and Helmchen, F. (2019).
779 Layer-specific integration of locomotion and sensory information in mouse barrel cortex. *Nat.*
780 *Commun.* 10, 2585.
- 781 Baker, M. (2016). 1,500 scientists lift the lid on reproducibility. *Nat. News* 533, 452.
- 782 Bari, A., Dalley, J.W., and Robbins, T.W. (2008). The application of the 5-choice serial
783 reaction time task for the assessment of visual attentional processes and impulse control in
784 rats. *Nat. Protoc.* 3, 759–767.
- 785 Barros, A.C.B. de, Baruchin, L.J., Panayi, M.C., Nyberg, N., Samborska, V., Mealing, M.T.,
786 Akam, T., Kwag, J., Bannerman, D.M., and Kohl, M.M. (2021). Retrosplenial cortex is
787 necessary for spatial and non-spatial latent learning in mice.
- 788 Bhagat, J., Wells, M.J., Harris, K.D., Carandini, M., and Burgess, C.P. (2020). Rigbox: An
789 Open-Source Toolbox for Probing Neurons and Behavior. *ENeuro* 7.
- 790 Blanco-Pozo, M., Akam, T., and Walton, M. (2021). Dopamine reports reward prediction
791 errors, but does not update policy, during inference-guided choice.
- 792 Buscher, N., Ojeda, A., Francoeur, M., Hulyalkar, S., Claros, C., Tang, T., Terry, A., Gupta,
793 A., Fakhraei, L., and Ramanathan, D.S. (2020). Open-source raspberry Pi-based operant
794 box for translational behavioral testing in rodents. *J. Neurosci. Methods* 342, 108761.
- 795 Carli, M., Robbins, T.W., Evenden, J.L., and Everitt, B.J. (1983). Effects of lesions to
796 ascending noradrenergic neurones on performance of a 5-choice serial reaction task in rats;
797 implications for theories of dorsal noradrenergic bundle function based on selective attention
798 and arousal. *Behav. Brain Res.* 9, 361–380.
- 799 Chagas, A.M. (2018). Haves and have nots must find a better way: The case for open
800 scientific hardware. *PLOS Biol.* 16, e3000014.
- 801 Chong, E.Z., Panniello, M., Barreiros, I., Kohl, M.M., and Booth, M.J. (2019). Quasi-
802 simultaneous multiplane calcium imaging of neuronal circuits. *Biomed. Opt. Express* 10,
803 267–282.
- 804 Devarakonda, K., Nguyen, K.P., and Kravitz, A.V. (2016). ROBucket: A low cost operant
805 chamber based on the Arduino microcontroller. *Behav. Res. Methods* 48, 503–509.
- 806 Fitzpatrick, C.M., and Andreasen, J.T. (2019). Differential effects of ADHD medications on
807 impulsive action in the mouse 5-choice serial reaction time task. *Eur. J. Pharmacol.* 847,
808 123–129.
- 809 Grimm, C.M., Aksamaz, S., Schulz, S., Teutsch, J., Sicinski, P., Liss, B., and Kätzel, D.
810 (2018). Schizophrenia-related cognitive dysfunction in the Cyclin-D2 knockout mouse model
811 of ventral hippocampal hyperactivity. *Transl. Psychiatry* 8, 1–16.
- 812 Gurley, K. (2019). Two open source designs for a low-cost operant chamber using
813 Raspberry Pi™. *J. Exp. Anal. Behav.* 111, 508–518.

- 814 International Brain Laboratory, Aguillon-Rodriguez, V., Angelaki, D.E., Bayer, H.M.,
815 Bonacchi, N., Carandini, M., Cazes, F., Chapuis, G.A., Churchland, A.K., Dan, Y., et al.
816 (2020). A standardized and reproducible method to measure decision-making in mice.
817 BioRxiv 2020.01.17.909838.
- 818 Kilonzo, K., van der Veen, B., Teutsch, J., Schulz, S., Kapanaiyah, S.K.T., Liss, B., and
819 Kätzel, D. (2021). Delayed-matching-to-position working memory in mice relies on NMDA-
820 receptors in prefrontal pyramidal cells. *Sci. Rep.* 11, 8788.
- 821 Kim, B., Kenchappa, S.C., Sunkara, A., Chang, T.-Y., Thompson, L., Doudlah, R., and
822 Rosenberg, A. (2019). Real-time experimental control using network-based parallel
823 processing. *ELife* 8, e40231.
- 824 Koralek, A.C., and Costa, R.M. (2020). Sustained dopaminergic plateaus and noradrenergic
825 depressions mediate dissociable aspects of exploitative states. BioRxiv 822650.
- 826 Korn, C., Akam, T., Jensen, K.H.R., Vagnoni, C., Huber, A., Tunbridge, E.M., and Walton,
827 M.E. (2021). Distinct roles for dopamine clearance mechanisms in regulating behavioral
828 flexibility. *Mol. Psychiatry*.
- 829 Krakauer, J.W., Ghazanfar, A.A., Gomez-Marín, A., MacIver, M.A., and Poeppel, D. (2017).
830 Neuroscience Needs Behavior: Correcting a Reductionist Bias. *Neuron* 93, 480–490.
- 831 Lopes, G., Bonacchi, N., Frazão, J., Neto, J.P., Atallah, B.V., Soares, S., Moreira, L., Matias,
832 S., Itskov, P.M., Correia, P.A., et al. (2015). Bonsai: an event-based framework for
833 processing and controlling data streams. *Front. Neuroinformatics* 9.
- 834 Marder, E. (2013). The haves and the have nots. *ELife* 2, e01515.
- 835 Márquez, C., Rennie, S.M., Costa, D.F., and Moita, M.A. (2015). Prosocial Choice in Rats
836 Depends on Food-Seeking Behavior Displayed by Recipients. *Curr. Biol.* 25, 1736–1745.
- 837 Navarra, R., Graf, R., Huang, Y., Logue, S., Comery, T., Hughes, Z., and Day, M. (2008).
838 Effects of atomoxetine and methylphenidate on attention and impulsivity in the 5-choice
839 serial reaction time test. *Prog. Neuropsychopharmacol. Biol. Psychiatry* 32, 34–41.
- 840 Nelson, A., Abdelmesih, B., and Costa, R.M. (2020). Corticospinal neurons encode complex
841 motor signals that are broadcast to dichotomous striatal circuits. BioRxiv
842 2020.08.31.275180.
- 843 O'Connor, D.H., Clack, N.G., Huber, D., Komiyama, T., Myers, E.W., and Svoboda, K.
844 (2010). Vibrissa-Based Object Localization in Head-Fixed Mice. *J. Neurosci.* 30, 1947–1967.
- 845 O'Leary, J.D., O'Leary, O.F., Cryan, J.F., and Nolan, Y.M. (2018). A low-cost touchscreen
846 operant chamber using a Raspberry Pi™. *Behav. Res. Methods* 50, 2523–2530.
- 847 Paterson, N.E., Ricciardi, J., Wetzler, C., and Hanania, T. (2011). Sub-optimal performance
848 in the 5-choice serial reaction time task in rats was sensitive to methylphenidate,
849 atomoxetine and d-amphetamine, but unaffected by the COMT inhibitor tolcapone. *Neurosci.*
850 *Res.* 69, 41–50.
- 851 Pillidge, K., Porter, A.J., Vasili, T., Heal, D.J., and Stanford, S.C. (2014). Atomoxetine
852 reduces hyperactive/impulsive behaviours in neurokinin-1 receptor 'knockout' mice.
853 *Pharmacol. Biochem. Behav.* 127, 56–61.

- 854 Samborska, V., Butler, J.L., Walton, M.E., Behrens, T.E., and Akam, T. (2021).
855 Complementary Task Representations in Hippocampus and Prefrontal Cortex for
856 Generalising the Structure of Problems. *BioRxiv* 2021.03.05.433967.
- 857 Saunders, J.L., and Wehr, M. (2019). Autopilot: Automating behavioral experiments with lots
858 of Raspberry Pis. *BioRxiv* 807693.
- 859 Strahnen, D., Kapanaiiah, S.K.T., Bygrave, A.M., Liss, B., Bannerman, D.M., Akam, T.,
860 Grewe, B.F., Johnson, E.L., and Kätzel, D. (2021). Highly task-specific and distributed neural
861 connectivity in working memory revealed by single-trial decoding in mice and humans.
- 862 van der Veen, B., Kapanaiiah, S.K.T., Kilonzo, K., Steele-Perkins, P., Jendryka, M.M.,
863 Schulz, S., Tasic, B., Yao, Z., Zeng, H., Akam, T., et al. (2021). Control of impulsivity by Gi-
864 protein signalling in layer-5 pyramidal neurons of the anterior cingulate cortex. *Commun.*
865 *Biol.* 4, 1–16.
- 866
- 867

868 **Supplementary Figures**

```
I Experiment name : run_task
I Task name : example_task
I Task file hash : 2791769213
I Setup ID : COM1
I Subject ID : m001
I Start date : 2021/09/17 10:30:59

S {"LED_on": 1, "LED_off": 2}

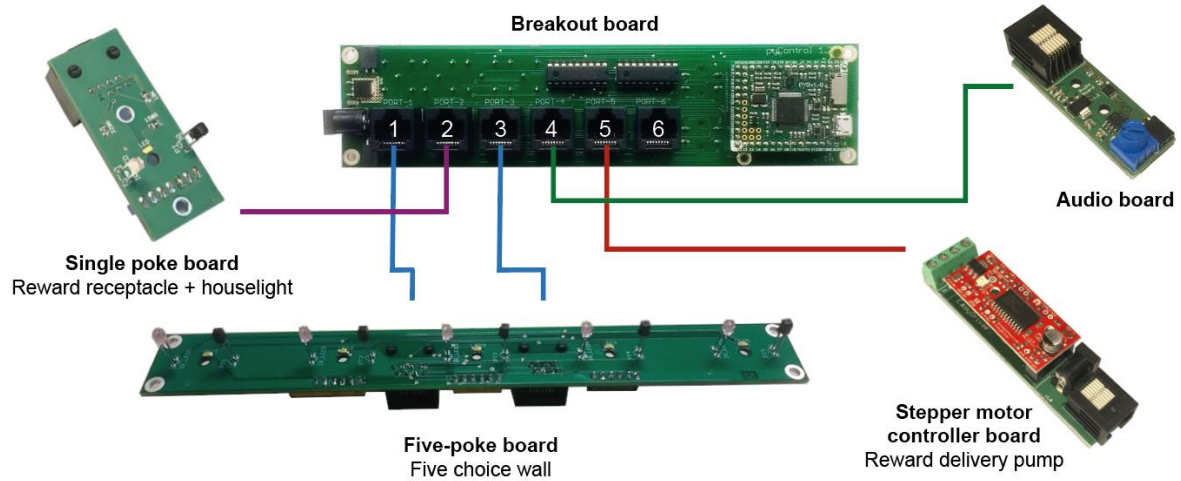
E {"button_press": 3}

D 0 2
D 2699 3
P 2700 Press number 1
D 4879 3
P 4880 Press number 2
D 5340 3
P 5341 Press number 3
D 5341 1
D 6341 2
V 13463 press_n 2
D 20338 3
P 20339 Press number 3
D 20339 1
D 21339 2
```

869 **Figure S1 (related to figure 1). Example data file.** Text file generated by running the example task
870 shown in figure 1. Lines beginning I contain information about the session including subject, task and
871 experiment names, start date and time. The single line beginning S is a JSON object (also a Python
872 dict) containing the state names and corresponding IDs used below in the data file. The single line
873 beginning E is a JSON object containing the event names and corresponding IDs. Lines beginning D
874 are data lines generated while the framework was running, with format `D timestamp ID` where
875 timestamp is the time in milliseconds since the start of the framework run and ID is a state ID
876 (indicating a state transition) or an event ID (indicating an event occurred). Lines beginning P are the
877 output of print statements with format `P timestamp printed output`. The line beginning V indicates the
878 value of a task variable that has been set by the user while the task was running, along with a
879 timestamp.

880

881



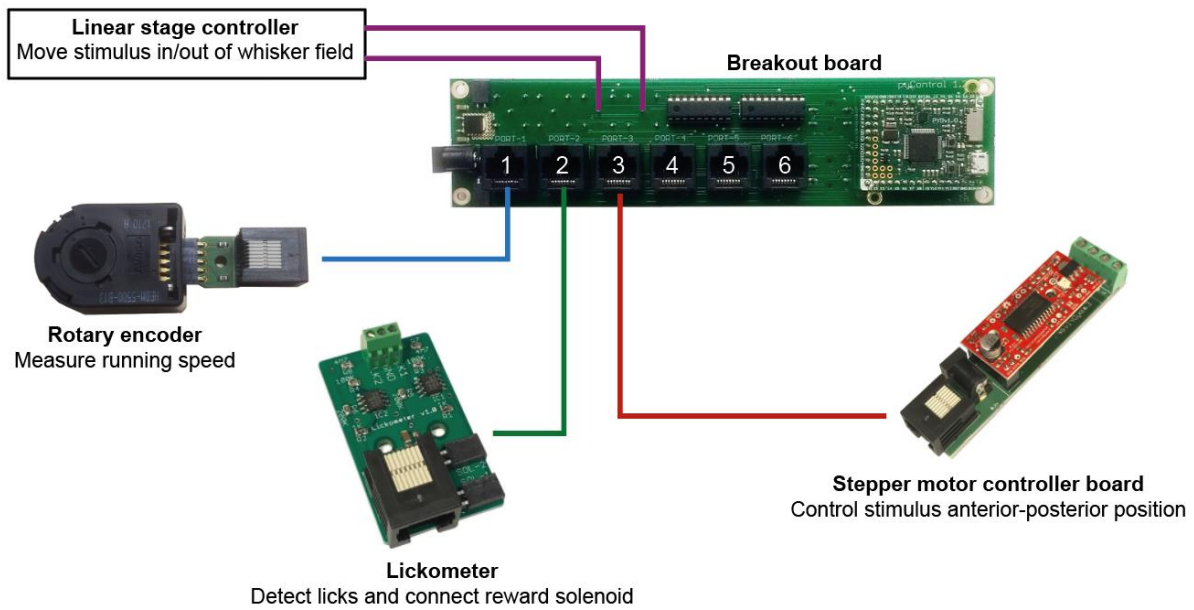
882

883 **Figure S2 (related to figure 6). Hardware configuration for 5-choice serial reaction time task.**

884 Diagram of hardware modules used to implement the 5-CSRT task. A breakout board is connected to
885 a Five-poke board which integrates the IR beams and LEDs for the ports on the 5 choice wall onto a
886 single PCB controlled from two behaviour ports, a stepper motor controller is used with a custom
887 made 3D printed peristaltic pump for reward delivery, a single poke board is used for the reward
888 receptacle with a 12v LED module used for house light connected to its solenoid output connector,
889 and an audio board for generating auditory stimuli. The hardware definition for this setup is provided
890 in the manuscript's code repository ([link](#)).

891

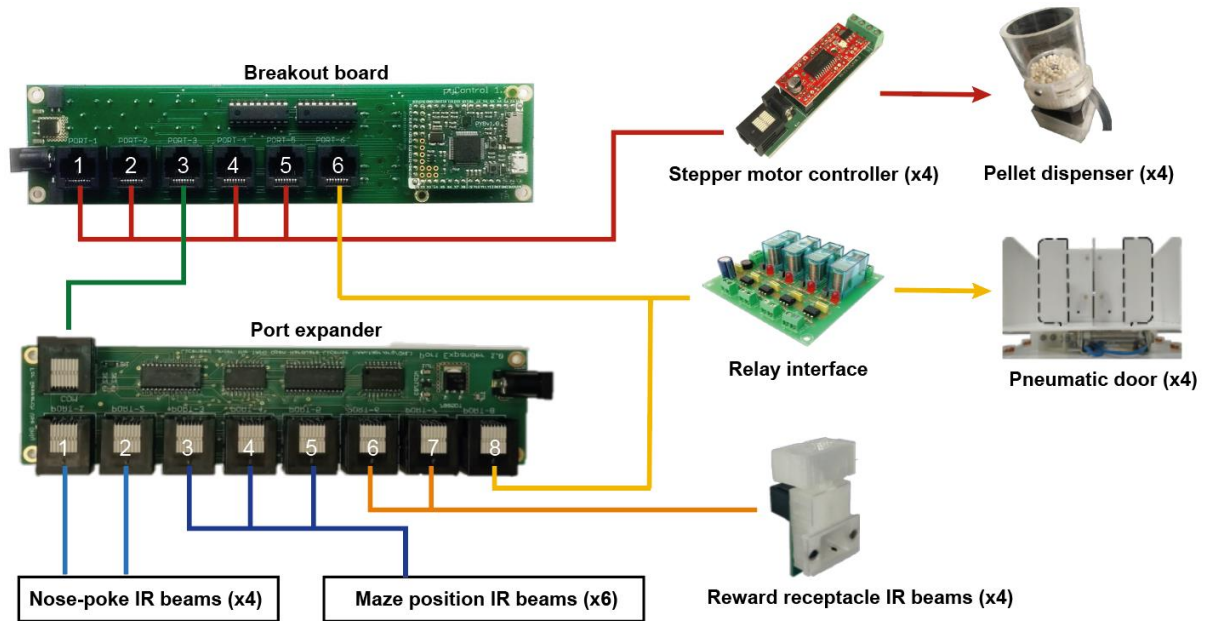
892



893

894 **Figure S3 (related to figure 7). Hardware configuration for vibrissae-based object localisation**
895 **task.** Diagram of the hardware modules used to implement the head-fixed vibrissae-based object
896 localisation task. A breakout board is connected to a rotary encoder module, used to measure running
897 speed, a lickometer, used to detect licks and control the reward solenoid, a stepper motor controller
898 used to set the anterior-posterior position of the stimulus, and a controller for the linear stage used to
899 move the stimulus in and out of the whisker field. The hardware definition for this setup is provided in
900 the manuscript's code repository ([link](#)).

901



902

903

904

905

906

907

908

Figure S4 (related to figure 8). Hardware configuration for social decision making task. Diagram of the hardware modules used to implement the double T maze apparatus for the social decision making task. A port expander is used to provide additional IO lines for IR beams, stepper motor controller boards are used to control custom made pellet dispensers, and a relay interface board is used to control the solenoids actuating the pneumatic doors. The hardware definition for this setup is provided in the manuscript's code repository ([link](#)).